

Cite this: *Chem. Sci.*, 2020, 11, 2479

All publication charges for this article have been paid for by the Royal Society of Chemistry

Received 10th December 2019  
Accepted 24th January 2020

DOI: 10.1039/c9sc06239d

rsc.li/chemical-science

## Radical cascade synthesis of azoles via tandem hydrogen atom transfer†

Andrew D. Chen,<sup>‡</sup> James H. Herbort,<sup>‡</sup> Ethan A. Wappes, Kohki M. Nakafuku, Darsheed N. Mustafa and David A. Nagib<sup>†\*</sup>

A radical cascade strategy for the modular synthesis of five-membered heteroarenes (e.g. oxazoles, imidazoles) from feedstock reagents (e.g. alcohols, amines, nitriles) has been developed. This double C–H oxidation is enabled by *in situ* generated imidate and acyloxy radicals, which afford regio- and chemo-selective  $\beta$  C–H bis-functionalization. The broad synthetic utility of this tandem hydrogen atom transfer (HAT) approach to access azoles is included, along with experiments and computations that provide insight into the selectivity and mechanism of both HAT events.

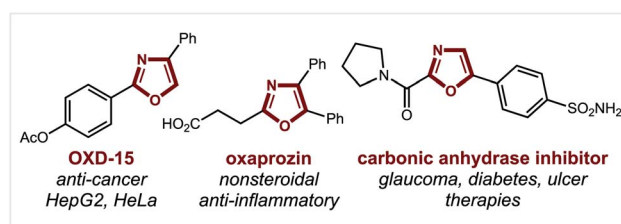
### Introduction

Nitrogen-containing heterocycles are prevalent in medicinal chemistry.<sup>1</sup> Specifically, five-membered heteroaromatics, such as oxazoles, imidazoles, and thiazoles, are among the most common structures found in drugs.<sup>2</sup> These azoles mimic biological interactions while also providing increased metabolic stability.<sup>3</sup> Such privileged medicinal motifs are typically synthesized from analogs of amines and carbonyls (Fig. 1a).<sup>4</sup> Alternatively, we envisioned a complementary synthetic route might entail direct combination of alcohols and nitriles through a double hydrogen atom transfer (HAT) mechanism (Fig. 1b). In this proposal, an imidate may undergo a tandem HAT sequence, which includes  $\beta$  C–H amination and subsequent aromatization of a transient oxazoline, to afford an oxazole. Recently, we disclosed a radical-mediated  $\beta$  C–H amination of imidates<sup>5,6</sup> to afford oxazolines *via* regioselective HAT.<sup>7,8</sup> Subsequently, the oxazoline was oxidized to a heteroarene (*i.e.* oxazole) in a post-synthetic operation. Given the pharmacological value of azoles, as well as the broad availability<sup>9</sup> of the feedstock reagents used in this C–H amination strategy, we questioned if we could streamline the multi-step, imidate radical-mediated strategy into a single, tandem HAT sequence.

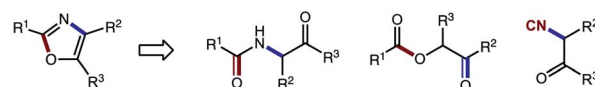
In our previous approach, we prepared aryl imidates by a two-step protocol (Fig. 2a), entailing temporary addition of trifluoroethanol to benzonitrile followed by transimidation with the desired alcohol.<sup>5</sup> The imidate was then converted to an oxazole *via* a second, two-step protocol (Fig. 2b), entailing  $\beta$  C–H

amination to form an oxazoline, followed by oxidative aromatization with DDQ. A limitation of this strategy is each of these four steps was carried out sequentially, and involved discrete isolation and purification by column chromatography.

Moreover, although  $\beta$  C–H amination is viable with electronically distinct classes of imidates (R = CCl<sub>3</sub>, Ph), only the former variant may be converted to an oxazole (76% yield). Conversely, the more generalizable, aryl oxazolines are



#### a. Classic oxazole synthons: carbonyl condensation reactions



#### b. Design: Azole synthesis via $\beta$ C–H amination radical cascade

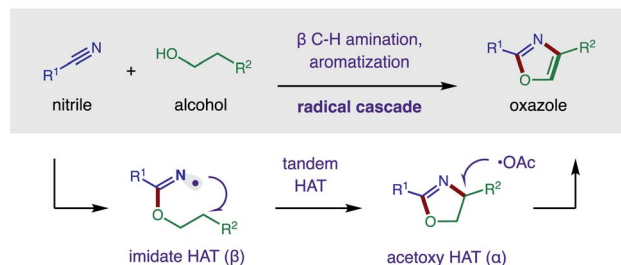


Fig. 1 Azole synthesis *via* (a) classic strategies, or (b) tandem hydrogen atom transfer.

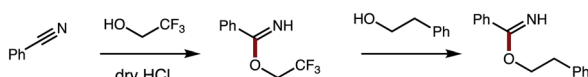
Department of Chemistry and Biochemistry, The Ohio State University, Columbus, OH 43210, USA. E-mail: nagib.1@osu.edu

† Electronic supplementary information (ESI) available. See DOI: 10.1039/c9sc06239d

‡ These authors contributed equally.



## a. Indirect transimidation (2 steps)



## b. Sequential oxidations (2 steps; limitations for step 2)

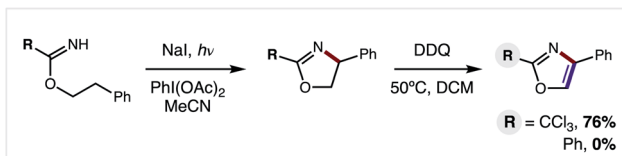


Fig. 2 Previous 4-step approach entails: (a) 2-step imidate synthesis, and (b) 2-step oxidation, limited to  $R = \text{CCl}_3$ .

oxidatively decomposed by DDQ – affording 0% oxazole (see ESI for details†). Thus, to improve this strategy and significantly expand its scope, we sought to prepare benzimidates in a single step (*versus* the two-step, transimidation route). Importantly, we also postulated that the two C–H oxidations could be performed in a single, tandem oxidative transformation (*cf.* Fig. 1b).

## Results and discussion

Toward a more streamlined approach (Fig. 3), we developed a method for preparing benzimidates directly by combining alcohols, nitriles, and triflic acid. This route is significantly more efficient (**1**, 99% conversion, 85% yield) and no longer requires gaseous HCl or sacrificial trifluoroethanol. As an added benefit, these triflate salts are isolable by crystallization (and basic work-up) – precluding the need for column chromatography.

With this one-step protocol for accessing imidates in hand, we then tested our proposal for direct conversion of the imidate to an oxazole *via* tandem C–H oxidation. One of our key findings was that solvent plays a crucial role in promoting double HAT (Table 1). For example,  $\beta$  C–H amination of benzimidate **1** affords oxazoline **2** quantitatively in MeCN. To our surprise, less polar solvents (*e.g.* DCE, PhMe) facilitate a *second* HAT as well, to enable direct formation of oxazole **3** (entries 1–3). Given the limited solubility of alkali iodide salts, other cations were investigated (entries 4–6) with the larger CsI emerging as the most efficient reagent. Control reactions indicate the double oxidation may be initiated with other visible light sources or in the dark – albeit with decreased efficiency (entries 7–9). Interestingly, while our previous

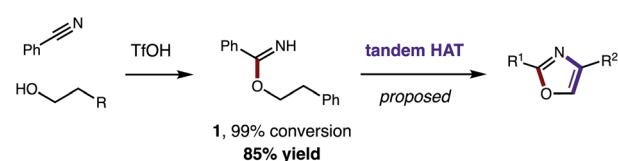


Fig. 3 Streamlined access to azoles from alcohols and nitriles (by direct synthesis of benzimidates and tandem HAT).

Table 1 Development of a tandem HAT-mediated synthesis of an oxazole<sup>a</sup>

Entry	MI	Solvent	$h\nu$	Yield <b>2</b>	Yield <b>3</b>
1	NaI	MeCN	23 W CFL	99%	0%
2	NaI	DCE	23 W CFL	35%	66%
3	NaI	PhMe	23 W CFL	15%	85%
4	KI	PhMe	23 W CFL	5%	76%
5	CsI	PhMe	23 W CFL	0%	98%
6	<sup>n</sup> Bu <sub>4</sub> I	PhMe	23 W CFL	25%	55%
7	CsI	PhMe	Blue LED	0%	82%
8	CsI	PhMe	Dark	75%	12%
9	CsI	PhMe	Dark, 50 °C	50%	35%
10	5% I <sub>2</sub>	PhMe	23 W CFL	58%	24%

<sup>a</sup> Conditions: imidate (0.2 mmol), MI (3 equiv.), PhI(OAc)<sub>2</sub> (3 equiv.), solvent (2 mL), 23 W compact fluorescent light (CFL), 23 °C, 24 h. <sup>1</sup>H NMR yields *vs.* standard.

catalytic I<sub>2</sub> conditions<sup>5b</sup> exclusively provide oxazoline in polar solvents (DMF, MeCN), 5% I<sub>2</sub> affords a 2 : 1 ratio of oxazole : oxazoline in PhMe (entry 10).

## Synthetic scope

Having developed an efficient, tandem oxidative method to enable  $\beta$  C–H amination and ensuing HAT to convert imidates

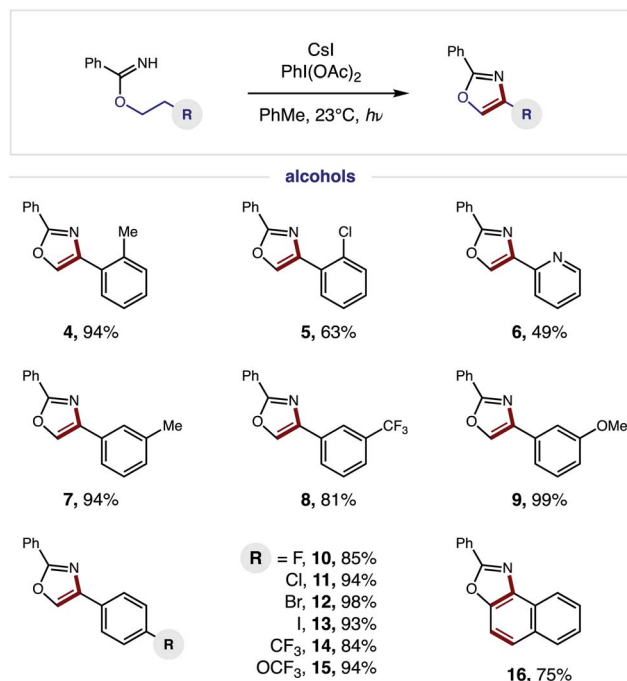


Fig. 4 Tandem HAT-mediated oxazole synthesis: alcohol scope.



to oxazoles, we next investigated the generality of this radical cascade. As shown in Fig. 4, a broad range of alcohols can be employed, including functional groups that are both electronically withdrawing and releasing. These diverse substituents may be at the *ortho* (4–5), *meta* (7–9), or *para* (10–15) positions of various 2-phenylethanol analogs.

Additionally, a pyridyl alcohol affords the privileged bis-heteroarene **6**, commonly employed as a chelating ligand in catalysis or as a drug fragment. Interestingly, the secondary alcohol, tetrahydronaphthalen-2-ol, undergoes a triple C–H oxidation, wherein formation of both a second and third aromatic ring affords naphthyl-fused oxazole **16**.

We next explored the generality of the nitrile component (Fig. 5). Since a broad range of sterically and electronically diverse nitriles are commercially available, we tested a variety of substitution patterns on the benzonitrile fragment. Again, OMe, CF<sub>3</sub>, and various halide substituents are well tolerated (**17–22**), indicating minimal effect of electronics on efficiency of the tandem oxidative protocol – albeit longer reaction times are required for electron-deficient imidates. Polyaromatic nitriles, including 1- and 2-naphthyls as well as 4-biphenyl, are also amenable to this oxidative cascade reaction to afford unique (hetero)polyarenes (**23–25**). Notably, this β C–H amination strategy does not afford over-halogenation – in contrast to the benzylic bromination of phenethyl amides, which exclusively yields bromo-oxazoles.<sup>10</sup>

### Synthetic applications

Having demonstrated broad synthetic utility of this radical cascade to access 2,4-bis-aryl-oxazoles, we questioned if this approach could also streamline entry to other classes of azoles

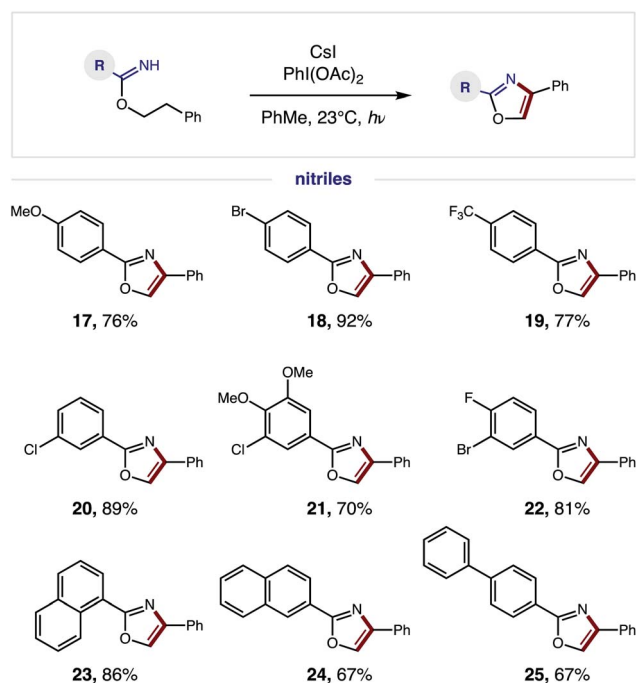


Fig. 5 Radical cascade oxazole synthesis: nitrile scope.

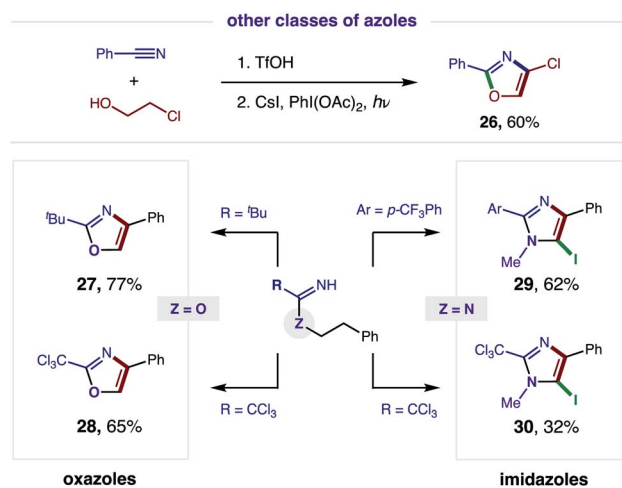


Fig. 6 Accessing a family of azoles via tandem HAT.

(Fig. 6). To this end, we subjected 2-Cl ethanol to our two-step sequence and were pleased to find the intermediate imidate is readily converted to the synthetically versatile 4-Cl oxazole (**26**) via double HAT. Next, we examined the aliphatic, pivalonitrile-derived imidate and found it cleanly affords 2-<sup>t</sup>Bu-oxazole (**27**). We also developed conditions for tandem β C–H oxidation of a trichloroacetimidate to its oxazole (**28**), precluding our previous need for oxazoline isolation and subsequent oxidation with DDQ.<sup>5a</sup>

We next sought to access imidazoles by subjecting amidines (Z = N) to this double HAT, wherein the key β C–H amination step was inspired by Chiba's Cu-catalyzed conversion of amidines to imidazolines.<sup>11</sup> To this end, we were pleased to find our imidate protocol also converts 2-Ar and 2-CCl<sub>3</sub> amidines to imidazoles (**29–30**). Interestingly, electrophilic aromatic iodination is also observed yielding 5-iodo-imidazoles via a triple C–H oxidation cascade. This third oxidation likely occurs in this case because imidazoles are more easily oxidized than oxazoles (by ~0.6 V).<sup>12</sup>

Since this new, two-step method affords a more rapid and modular route to azoles, which is ideal for medicinal chemistry

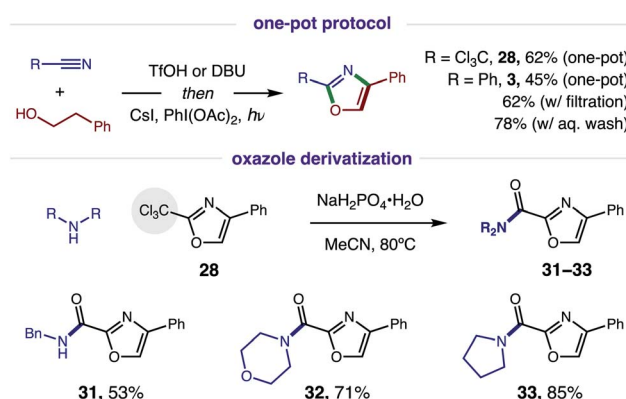


Fig. 7 Streamlined synthesis via one-pot protocol, and utility of trichloromethyl oxazoles.



applications, we tested the viability of a one-pot protocol for combining these modular, feedstock components (*e.g.* alcohol, nitrile) and converting the resulting imidate to oxazoles (Fig. 7). To our delight, this further streamlined method readily affords both classes of oxazoles ( $R = \text{CCl}_3$  **28**, 62%; Ph, **3**, 45%) directly from an alcohol and nitrile. In the less efficient case (**3**), we found the one-pot procedure can be improved by filtration of the imidate hydrotriflate salt intermediate to remove excess TfOH (62%). Alternatively, basic, aqueous wash of the imidate affords greatest efficiency (78%). Given a maximum, theoretical yield of 80% for imidate formation, these tandem oxidations are achieved in 78% and 98% yields, respectively. We anticipate the latter approach will be the preferred method for constructing oxazole libraries for medicinal chemistry applications.

Intrigued by the possibility of derivatizing 2- $\text{CCl}_3$  oxazoles to other drug-like motifs, we subjected **28** to nucleophilic addition by a variety of amines. Although expecting an addition-elimination mechanism<sup>13</sup> to displace  $\text{CCl}_3$  by amines, we were surprised to find that amides **31–33** were instead obtained *via* Cl-displacement and ensuing hydrolysis of the remaining *gem*-dichloride. We expect these electron-deficient oxazole amides to exhibit greater metabolic stability as potential drug fragments.<sup>3</sup> Notably, these motifs have already shown efficacy as carbonic anhydrase inhibitors (*cf.* Fig. 1).

### Mechanistic investigations

Our proposed mechanism for the radical cascade conversion of imidate **A** (from addition of an alcohol and nitrile) to an oxazole is shown in Fig. 8. To start, *in situ* combination of CsI and  $\text{PhI}(\text{OAc})_2$  affords AcOI, which serves as an electrophilic iodine source.<sup>14</sup> Upon combination with imidate **A**, an *N*-iodo imidate **B** is transiently formed. In the presence of visible light, homolysis of the weak N–I bond (N–I BDFE;  $23.0 \text{ kcal mol}^{-1}$ )<sup>15</sup> generates N-centered imidate radical **C**, which initiates a regioselective  $\beta$  C–H amination *via* 1,5-HAT to afford C-centered radical **D** ( $\Delta G = -6.2 \text{ kcal mol}^{-1}$ ;  $\Delta G^\ddagger = +14.3 \text{ kcal mol}^{-1}$ ).<sup>16</sup> The combination of this alkyl radical with an iodine atom ( $\text{I}^\cdot$ ; or

AcOI,  $\text{I}_2$ , **B**) provides  $\beta$  iodide **E**. Spontaneous cyclization under these conditions affords oxazoline **F**. At this point, a second HAT likely occurs *via*  $\alpha$ -imino C–H abstraction (C–H BDFE;  $64.8 \text{ kcal mol}^{-1}$ ) by an electrophilic O-centered acyloxy radical ( $\text{AcO}^\cdot$  derived from AcOI) to afford AcOH (O–H BDFE;  $98.7 \text{ kcal mol}^{-1}$ ) and  $\alpha$ -imino radical **G**.<sup>15</sup> This previously undetected second HAT is both thermodynamically favored and kinetically feasible ( $\Delta G = -32.8 \text{ kcal mol}^{-1}$ ;  $\Delta G^\ddagger = +4.9 \text{ kcal mol}^{-1}$ ), according to DFT calculations (details below).<sup>16</sup> Combination of  $\alpha$ -imino radical **G** with an iodine donor (*e.g.*  $\text{I}^\cdot$ , AcOI,  $\text{I}_2$ , **B**) then provides  $\alpha$ -iodide **H**. Finally, aromatization by loss of HI affords oxazole **I** as a final step in this cascade mechanism.<sup>17</sup>

As noted above, solvent polarity is crucial in mediating the second HAT. A likely explanation is that decarboxylation of the  $\text{H}^\cdot$  abstracting reagent,  $\text{AcO}^\cdot$ , to a less efficient HAT mediator,  $\text{Me}^\cdot$ , is rapid in polar solvents (MeCN), whereas bimolecular HAT may outcompete this  $\beta$  scission in non-polar solvents (PhMe).<sup>18</sup>

To further evaluate the proposed tandem HAT mechanism, we probed a possibility that solvent does not inhibit the second HAT, but instead prevents conversion of  $\alpha$ -imino radical **G** to oxazole by back-HAT from solvent to regenerate the oxazoline (Fig. 9a). To test this hypothesis, oxazoline **2** was prepared and subjected to standard conditions (PhMe, 24 h). The resulting quantitative conversion to oxazole **3** supports the intermediacy of oxazoline **F**. Next, interrupting the reaction at 5 h in  $d_8$ -PhMe affords incomplete conversion (43% **3**) with no deuteration of the remaining oxazoline – indicating deleterious back-HAT from solvent is not operative. Similarly,  $d_3$ -MeCN affords 10%

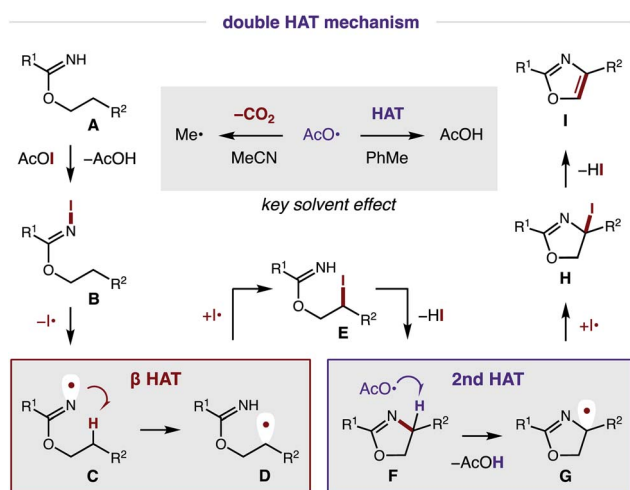


Fig. 8 Proposed mechanism and rationale for solvent effect.

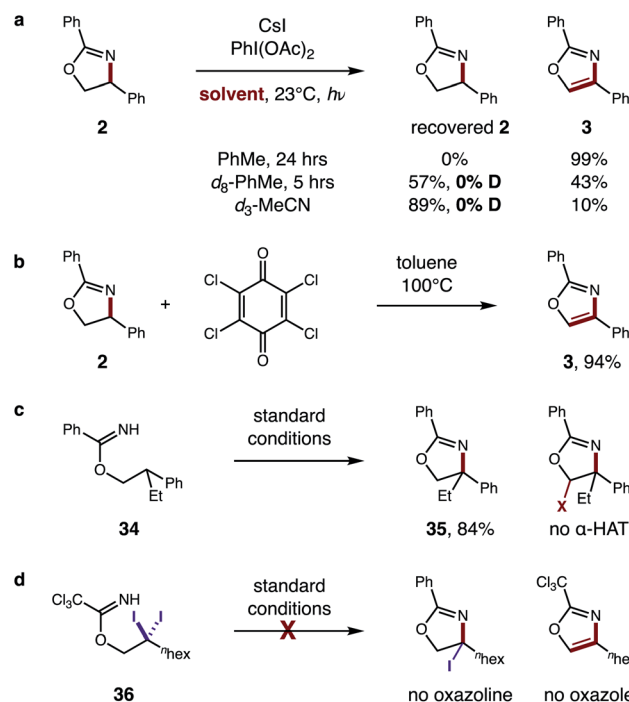


Fig. 9 Mechanistic evaluation of second HAT. (a) Intermediate evaluation and deuterium experiments. (b) Benzylic oxidation. (c) HAT regioselectivity. (d) Alternate pathway.





3, but no deuterated oxazoline, suggesting the 89% recovered 2 is more likely a result of inhibited HAT rather than back-HAT. Benzylic oxidation of oxazoline 2 by chloranil, albeit under harsher conditions (100 °C), also affords oxazole 3 (94%), providing further support for this cascade oxidation pathway (Fig. 9b).

To probe the regioselectivity of the proposed second HAT,  $\beta$  di-substituted imidate 34 was prepared and subjected to standard conditions (Fig. 9c). Since the resulting oxazoline 35 contains no  $\alpha$ -imino C–H, its efficient formation (84%) and the absence of any further  $\alpha$ -oxy oxidation supports the predicted regioselectivity of the second HAT. Finally, an alternate mechanism was also investigated (Fig. 9d), entailing  $\beta$  C–H di-halogenation<sup>6a</sup> followed by subsequent displacement and elimination of the halides to form oxazole. Yet, when subjecting

$\beta$  gem-di-iodide 36 to reaction conditions, neither an oxazole nor oxazoline product is observed.

In addition to strong solvent effects, we also observed interesting stereoelectronic influences on the second HAT step (Fig. 10). In particular, large steric hindrance by highly withdrawing groups prevent aromatization to the oxazole. For example, a CF<sub>3</sub> substituent affords oxazoles efficiently when *meta* or *para*, but halts the mechanism at oxazoline 37 when at the *ortho* position. This contrasts with a CH<sub>3</sub> group, which affords oxazole cleanly – even when substituted at the *ortho* position (4). Additionally, acyclic, secondary alcohols exhibit significant steric inhibition for the second HAT. For example, under alternate conditions,<sup>5b</sup> 1-Ph-2-propanol imidate 38 affords a mixture of oxazoline diastereomers (1.4 : 1 *syn* : *anti*). However, upon subjecting oxazolines 39 (mixture of both isomers) to these reaction conditions, the *syn* isomer is readily converted to oxazole 40, while 75% of the *anti* isomer is recovered. As shown by a model in Fig. 10, the second HAT by AcO<sup>•</sup> is sterically inhibited in the case of the *anti* oxazoline. For a complete list of substrate limitations, see ESI Section X.†

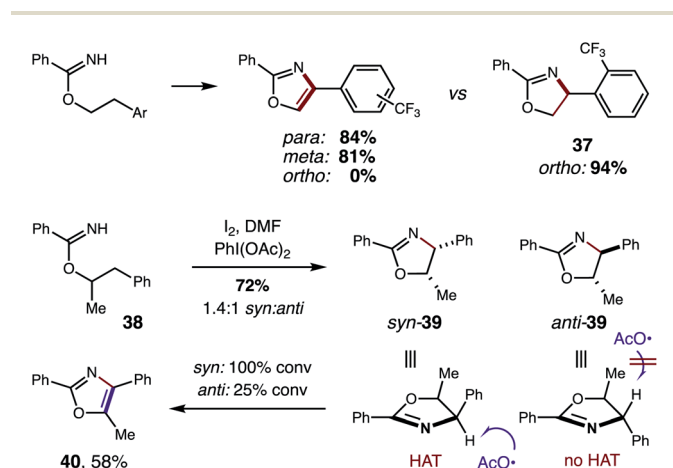


Fig. 10 Stereoelectronic effects on second HAT.

## Computations

DFT calculations were also performed to provide additional insights into the proposed double HAT cascade mechanism (Fig. 11). First, the free energy of each reaction intermediate was computed – from benzimidate I to oxazole IX. These results indicate the overall reaction is net exergonic ( $\Delta G_{\text{rxn}}^{\circ} = -70.1$  kcal mol<sup>-1</sup>). This is in addition to the energy released upon ligand exchange of CsI and PhI(OAc)<sub>2</sub> to form AcOI ( $\Delta G^{\circ} = -25.0$  kcal mol<sup>-1</sup>). The main contributors to the large thermodynamic driving force for this reaction are aromatization (to form IX) and net reduction of AcOI to AcOH (twice; with II and VII). On the other hand, the most endergonic

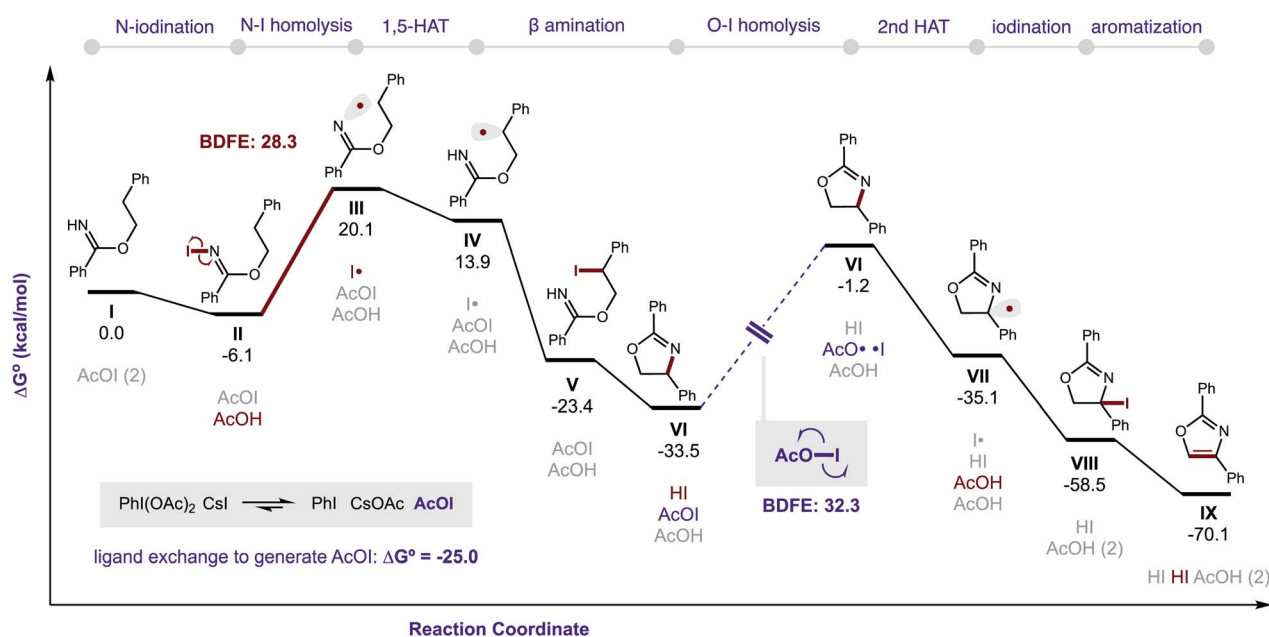


Fig. 11 Gibbs free energies of reaction intermediates. ωB97X-D/6-311++G(d,p)/Def2-TZVPP(I and Cs)/PCM(PhMe).



steps entail radical formation. Specifically, toward generation of the N-centered radical, iodination of imidate **I** to **II** is slightly exergonic ( $\Delta G = -6 \text{ kcal mol}^{-1}$ ), but subsequent homolysis of **II** to **III** is much more endergonic ( $\Delta G = 26 \text{ kcal mol}^{-1}$ ) – correlating to an N–I BDFE of  $28 \text{ kcal mol}^{-1}$ . Similarly, O–I homolysis (to generate  $\text{AcO}^\bullet$  from  $\text{AcOI}$ ) is highly endergonic (BDFE =  $32 \text{ kcal mol}^{-1}$ ), which corresponds to the large  $\Delta G$  for **VI** (and intermediates) in the reaction coordinate diagram prior to the second HAT. Notably, applying implicit solvent models (that largely rely on field-based effects such as dielectric constant) to both the decarboxylation and second HAT pathways does not explain the experimentally observed solvent effects.

Additional calculations were performed to provide further insight into the key HAT steps of the reaction mechanism (Fig. 12a). First, 1,5-HAT of imidate radical **III** to  $\beta$ -carbon radical **IV** via **IV-TS(1,5)** was found to be kinetically feasible ( $\Delta G^\ddagger = 14.3 \text{ kcal mol}^{-1}$ ) and thermodynamically downhill ( $\Delta G_{\text{rxn}}^\circ = -6.2 \text{ kcal mol}^{-1}$ ). Next, probing the energetics behind the 1,5-HAT regioselectivity, an alternate 1,4-HAT pathway, **IV-TS(1,4)**, was found to be much less favoured – both kinetically ( $\Delta\Delta G^\ddagger = 5 \text{ kcal mol}^{-1}$ ) and thermodynamically ( $\Delta\Delta G_{\text{rxn}}^\circ = 6 \text{ kcal mol}^{-1}$ ). Additionally, the C–H bond length in transition state **IV-TS(1,5)** is closer to that of starting material **INT-III** (C–H: 1.27 vs. 1.09 Å, respectively) than the N–H bond of **IV-TS** is to product **INT-IV** (N–H: 1.32 vs. 1.02 Å, respectively), suggesting an early TS, which is consistent with 1,5-HAT being exergonic.

Importantly, we also investigated the second, intermolecular HAT in order to determine the nature and selectivity of this second C–H functionalization (Fig. 12b). Given the presence of

several species in the reaction medium that could promote intermolecular HAT of oxazoline **VI** (e.g.  $\text{I}^\bullet$ ,  $\text{AcO}^\bullet$ ,  $\text{Me}^\bullet$ ), we individually computed each possible pathway. Among these, HAT by  $\text{I}^\bullet$  was found to have the lowest kinetic barrier (**VII-TS(I)**,  $\Delta G^\ddagger = 6.0 \text{ kcal mol}^{-1}$ ), but results in the least exergonic pathway (**VII(I)**,  $\Delta G_{\text{rxn}}^\circ = -5.0 \text{ kcal mol}^{-1}$ ). Thus, whereas HAT by  $\text{I}^\bullet$  is feasible, the reverse reaction would be competitive. On the other hand,  $\text{AcO}^\bullet$  mediated HAT was determined to be next most accessible, kinetically (**VII-TS(OAc)**,  $\Delta G^\ddagger = 8.3 \text{ kcal mol}^{-1}$ ), as well as the most exergonic (**VII(OAc)**,  $\Delta G^\circ = -33.9 \text{ kcal mol}^{-1}$ ). Thus, we expect HAT by  $\text{AcO}^\bullet$  to be substantially less reversible. We also probed HAT by  $\text{Me}^\bullet$  since these species are formed by  $\beta$ -fragmentation of acetoxy radicals. Whereas  $\text{Me}^\bullet$  to  $\text{Me-H}$  HAT is feasible, it is kinetically slower than  $\text{AcO}^\bullet$  (**VII-TS(Me)**,  $\Delta G^\ddagger = 11.9 \text{ vs. } 8.3 \text{ kcal mol}^{-1}$ ) and less exergonic (**VII(Me)**,  $\Delta G^\circ = -30.0 \text{ vs. } -33.9 \text{ kcal mol}^{-1}$ ). Lastly, we considered the possibility of intermolecular HAT by an imidate N-centered radical – albeit this scenario would necessitate intermolecular HAT to outcompete intramolecular HAT. Nevertheless, such a pathway was found to have the highest kinetic barrier ( $\Delta G^\ddagger = 15.9 \text{ kcal mol}^{-1}$ ), while being only moderately exergonic ( $\Delta G^\circ = -22.0 \text{ kcal mol}^{-1}$ ). In support of these calculations, the experimental addition of non-1,5-HAT-capable imidates lacking  $\beta$  hydrogens, does not improve reaction efficiency (see ESI, Section IX<sup>†</sup>). Collectively, these data suggest HAT by acetoxy radical is the most likely pathway, since  $\text{AcO}^\bullet$  is the second most reactive and first most exergonic.

Turning our attention to selectivity of C–H abstraction from the oxazoline, we considered a competitive HAT at the  $\alpha$ -oxygen C–H bond. Approach of  $\text{AcO}^\bullet$  was made from the sterically less hindered face, *trans* to the phenyl group. When compared to the

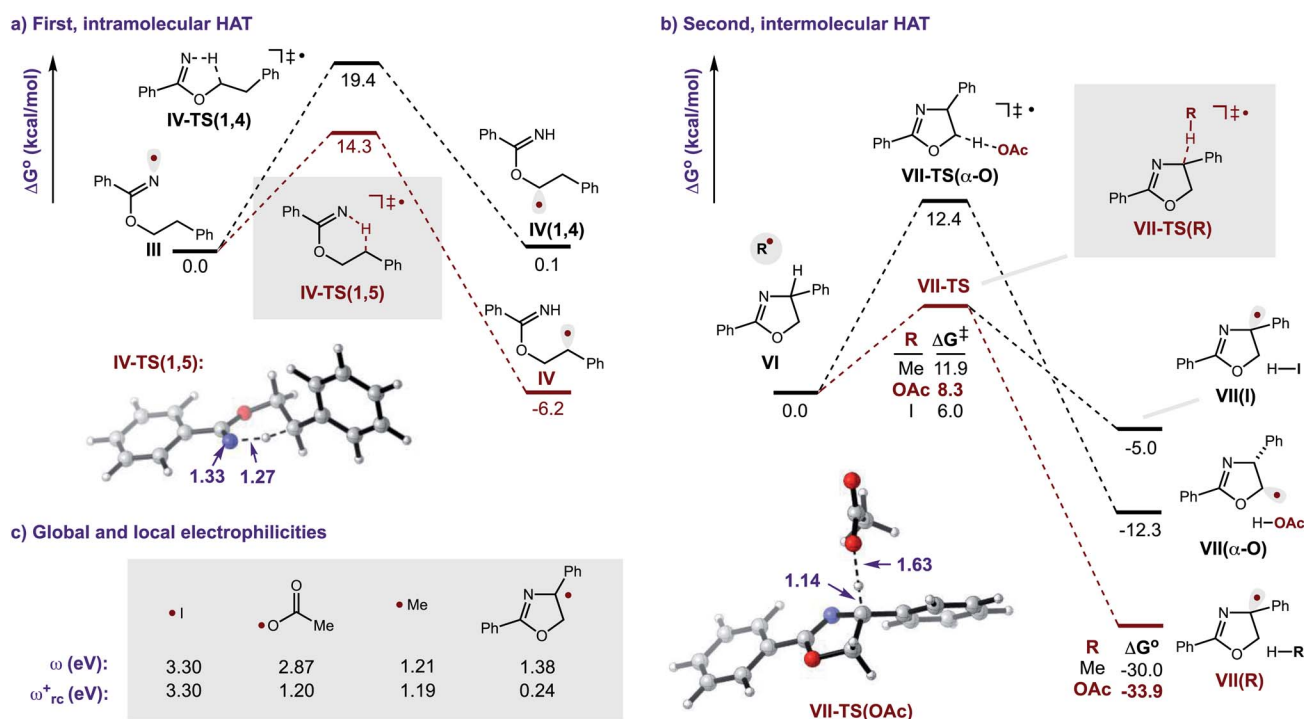


Fig. 12 Energetics of HAT steps. (a) 1,5 vs. 1,4 HAT. (b) Intermolecular HAT pathways. Selected TS bond lengths in angstroms, Å. (c) Global and local electrophilicities of key radicals.  $\omega_{\text{B97X-D/6-311++G(d,p)/Def2-TZVP(II)/PCM(PhMe)}$ .



$\alpha$ -imino C–H, this HAT is disfavoured, both kinetically (**VII-TS**( $\alpha$ -O),  $\Delta G^\ddagger = 12.4$  vs.  $8.3$  kcal mol<sup>-1</sup>) and thermodynamically (**VII**( $\alpha$ -O),  $\Delta G_{\text{rxn}}^\circ = -12.3$  vs.  $-33.9$  kcal mol<sup>-1</sup>).

Since kinetic reactivity of radicals are heavily influenced by their polarity,<sup>19</sup> we sought to account for these effects by calculating the global and local electrophilicities ( $\omega$  and  $\omega_{\text{rc}}^+$ , respectively) of the candidate H-abstractors (Fig. 12c). As radical **VII** (resulting from second HAT) is nucleophilic ( $\omega_{\text{rc}}^+ = 0.24$  eV), its generation is best matched with an electrophilic H-atom abstractor. Indeed, the relative order of kinetic reactivity was found to correlate with increasing local electrophilicity, from most to least reactive: iodine (3.30), acetoxy (1.20), methyl (1.19), and imidate (0.96). These data corroborate the free energy results that suggest AcO<sup>•</sup> is the likely mediator of the second HAT.

## Conclusions

In summary, a radical cascade strategy has enabled a streamlined, modular synthesis of azoles. This rapid approach for constructing molecular complexity from feedstock reagents is enabled by a tandem HAT mechanism. We expect the methods and mechanistic insights for this regio- and chemo-selective  $\beta$  C–H bis-functionalization presented herein will serve as a foundation for developing additional multi-component couplings based on radical-mediated C–H difunctionalization.

## Conflicts of interest

There are no conflicts to declare.

## Acknowledgements

We thank the National Institutes of Health (NIH R35 GM119812) National Science Foundation (NSF CAREER 1654656) and Sloan Foundation for financial support. We are grateful to Dr L.-C. Campeau (Merck) for an inspiring discussion on the synthesis and utility of azoles in medicine and to Remy F. Lalissee (OSU) for sharing computational expertise. High performance computing resources provided by The Ohio Supercomputer Center.

## Notes and references

- 1 E. Vitaku, D. T. Smith and J. T. Njardarson, *J. Med. Chem.*, 2014, **57**, 10257–10274.
- 2 M. D. Delost, D. T. Smith, B. J. Anderson and J. T. Njardarson, *J. Med. Chem.*, 2018, **61**, 10996–11020.
- 3 (a) D. J. S. Jean and C. Fotsch, *J. Med. Chem.*, 2012, **55**, 6002–6020; (b) N. A. Meanwell, *J. Med. Chem.*, 2011, **54**, 2529–2591.
- 4 (a) I. J. Turchi and M. J. S. Dewar, *Chem. Rev.*, 1975, **75**, 389–437; (b) B. H. Lipshutz, *Chem. Rev.*, 1986, **86**, 795–819; (c) S. D. Roughley and A. M. Jordan, *J. Med. Chem.*, 2011, **54**, 3451–3479.
- 5  $\beta$  C–H amination of imidates: (a) E. A. Wappes, K. M. Nakafuku and D. A. Nagib, *J. Am. Chem. Soc.*, 2017, **139**, 10204–10207; (b) L. M. Stateman, E. A. Wappes, K. M. Nakafuku, K. M. Edwards and D. A. Nagib, *Chem. Sci.*, 2019, **10**, 2693–2699.
- 6 Additional imidate radical transformations: (a) E. A. Wappes, A. Vanitcha and D. A. Nagib, *Chem. Sci.*, 2018, **9**, 4500–4504; (b) K. M. Nakafuku, S. C. Fosu and D. A. Nagib, *J. Am. Chem. Soc.*, 2018, **140**, 11202–11205; (c) X. Q. Mou, X. Y. Chen, G. Chen and G. He, *Chem. Commun.*, 2018, **54**, 515–518; (d) Y. Kumar, Y. Jaiswal and A. Kumar, *Org. Lett.*, 2018, **20**, 4964–4969; (e) F. Wang and S. S. Stahl, *Angew. Chem., Int. Ed.*, 2019, **58**, 6385–6390; (f) M. Shaw and A. Kumar, *Org. Lett.*, 2019, **21**, 3108–3113; (g) X.-Q. Mou, F.-M. Rong, H. Zhang, G. Chen and G. He, *Org. Lett.*, 2019, **21**(12), 4657–4661; (h) R. O. Torres-Ochoa, A. Leclair, Q. Wang and J. Zhu, *Chem.–Eur. J.*, 2019, **25**, 9477–9484.
- 7 HAT and C–H amination reviews: (a) L. M. Stateman, K. M. Nakafuku and D. A. Nagib, *Synthesis*, 2018, **50**, 1569–1586; (b) J. Robertson, J. Pillai and R. K. Lush, *Chem. Soc. Rev.*, 2001, **30**, 94–103; (c) Ž. Čeković, *Tetrahedron*, 2003, **59**, 8073–8090; (d) S. Z. Zard, *Chem. Soc. Rev.*, 2008, **37**, 1603–1618; (e) J. M. Mayer, *Acc. Chem. Res.*, 2011, **44**, 36–46; (f) J. L. Jeffrey and R. Sarpong, *Chem. Sci.*, 2013, **4**, 4092–4106; (g) S. Chiba and H. Chen, *Org. Biomol. Chem.*, 2014, **12**, 4051–4060; (h) M. Nechab, S. Mondal and M. P. Bertrand, *Chem.–Eur. J.*, 2014, **20**, 16034–16059; (i) J. R. Chen, X. Q. Hu, L. Q. Lu and W. J. Xiao, *Chem. Soc. Rev.*, 2016, **45**, 2044–2056; (j) T. Xiong and Q. Zhang, *Chem. Soc. Rev.*, 2016, **45**, 3069–3087; (k) W. Li, W. Xu, J. Xie, S. Yu and C. Zhu, *Chem. Soc. Rev.*, 2018, **47**, 654–667; (l) H. Zhang and A. Lei, *Synthesis*, 2019, **51**, 83–96.
- 8 Recent examples of HAT via N-centered radicals: (a) M. Yang, B. Su, Y. Wang, K. Chen, X. Jiang, Y.-F. Zhang, X.-S. Zhang, G. Chen, Y. Cheng, Z. Cao, Q.-Y. Guo, L. Wang and Z.-J. Shi, *Nat. Commun.*, 2014, **5**, 4707; (b) T. Liu, T.-S. Mei and J.-Q. Yu, *J. Am. Chem. Soc.*, 2015, **137**, 5871–5874; (c) C. Martínez and K. Muñiz, *Angew. Chem., Int. Ed.*, 2015, **54**, 8287–8291; (d) E. A. Wappes, S. C. Fosu, T. C. Chopko and D. A. Nagib, *Angew. Chem., Int. Ed.*, 2016, **55**, 9974–9978; (e) G. J. Choi, Q. Zhu, D. C. Miller, C. J. Gu and R. R. Knowles, *Nature*, 2016, **539**, 268–271; (f) J. C. K. Chu and T. Rovis, *Nature*, 2016, **539**, 272–275; (g) J. Ozawa, M. Tashiro, J. Ni, K. Oisaki and M. Kanai, *Chem. Sci.*, 2016, **7**, 1904–1909; (h) H. Lu, K. Lang, H. Jiang, L. Wojtas and X. P. Zhang, *Chem. Sci.*, 2016, **7**, 6934–6939; (i) D.-F. Chen, J. C. K. Chu and T. Rovis, *J. Am. Chem. Soc.*, 2017, **139**, 14897–14900; (j) T. Liu, M. C. Myers and J. Q. Yu, *Angew. Chem., Int. Ed.*, 2017, **56**, 306–309; (k) W. Shu and C. Nevado, *Angew. Chem., Int. Ed.*, 2017, **56**, 1881–1884; (l) W. Shu, A. Genoux, Z. Li and C. Nevado, *Angew. Chem., Int. Ed.*, 2017, **56**, 10521–10524; (m) R. Wang, Y. Li, R. X. Jin and X. S. Wang, *Chem. Sci.*, 2017, **8**, 3838–3842; (n) S. Liu, A. Liu, Y. Zhang and W. Wang, *Chem. Sci.*, 2017, **8**, 4044–4050; (o) M. A. Short, J. M. Blackburn and J. L. Roizen, *Angew. Chem., Int. Ed.*, 2018, **57**, 296–299; (p) E. M. Dauncey, S. P. Morcillo, J. J. Douglas, N. S. Sheikh and D. Leonori, *Angew. Chem., Int. Ed.*, 2018, **57**, 744–748; (q) S. P. Morcillo, E. M. Dauncey, J. H. Kim, J. J. Douglas, N. S. Sheikh and



- D. Leonori, *Angew. Chem., Int. Ed.*, 2018, **57**, 12945–12949; (r) Y. Xia, L. Wang and A. Studer, *Angew. Chem., Int. Ed.*, 2018, **57**, 12940–12944; (s) H. Jiang and A. Studer, *Angew. Chem., Int. Ed.*, 2018, **57**, 1692–1696; (t) C. G. Na and E. J. Alexanian, *Angew. Chem., Int. Ed.*, 2018, **57**, 13106–13109; (u) Z. Li, Q. Wang and J. Zhu, *Angew. Chem., Int. Ed.*, 2018, **57**, 13288–13292; (v) S. Sathyamoorthi, S. Banerjee, J. Du Bois, N. Z. Burns and R. N. Zare, *Chem. Sci.*, 2018, **9**, 100–104; (w) Y. Tang, Y. Qin, D. Meng, C. Li, J. Wei and M. Yang, *Chem. Sci.*, 2018, **9**, 6374–6378; (x) K. W. Bentley, K. A. Dummit and J. F. Van Humbeck, *Chem. Sci.*, 2018, **9**, 6440–6445; (y) T. Ide, J. P. Barham, M. Fujita, Y. Kawato, H. Egami and Y. Hamashima, *Chem. Sci.*, 2018, **9**, 8453–8460; (z) X. Bao, Q. Wang and J. Zhu, *Nat. Commun.*, 2019, **10**, 769; (aa) Z. Zhang, L. M. Stateman and D. A. Nagib, *Chem. Sci.*, 2019, **10**, 1207–1211; (ab) K. Wu, L. Wang, S. Colón-Rodríguez, G. U. Flechsig and T. Wang, *Angew. Chem., Int. Ed.*, 2019, **58**, 1774–1778; (ac) Z. Liu, H. Xiao, B. Zhang, H. Shen, L. Zhu and C. Li, *Angew. Chem., Int. Ed.*, 2019, **58**, 2510–2513; (ad) N. Tang, X. Wu and C. Zhu, *Chem. Sci.*, 2019, **10**, 6915–6919; (ae) A. Modak, E. N. Pinter and S. P. Cook, *J. Am. Chem. Soc.*, 2019, **141**, 18405; (af) Y. Qin, Y. Han, Y. Tang, J. Wei and M. Yang, *Chem. Sci.*, 2020, DOI: 10.1039/c9sc04169a.
- 9 See ESI† for analysis on abundance of nitriles, alcohols, and other feedstocks.
- 10 M. Dinda, S. Samanta, S. Eringathodi and P. K. Ghosh, *RSC Adv.*, 2014, **4**, 12252–12256.
- 11 (a) Y.-F. Wang, H. Chen, X. Zhu and S. Chiba, *J. Am. Chem. Soc.*, 2012, **134**, 11980–11983; (b) H. Chen, S. Sanjaya, Y.-F. Wang and S. Chiba, *Org. Lett.*, 2013, **15**, 212–215.
- 12 Calculated oxidation potentials (vs. SCE in MeCN): oxazole +2.64 V, imidazole +2.01 V.
- 13 R. P. Lester, T. Bham, T. W. Bousfield, W. Lewis and J. E. Camp, *J. Org. Chem.*, 2016, **81**, 12472–12477.
- 14 E. M. Chen, R. M. Keefer and L. J. Andrews, *J. Am. Chem. Soc.*, 1967, **89**, 428–430.
- 15 BDFE calculations of N–I, C–H, and O–H bonds, see ESI for more details.†
- 16 Calculations were performed at the  $\omega$ B97M-D/6-311++(d,p)/PCM(PhMe) level of theory.
- 17 Alternatively, outer-sphere oxidation to the benzylic carbocation and subsequent elimination may promote direct aromatization of radical **G** to oxazole **I**.
- 18 (a) P. S. Skell and D. D. May, *J. Am. Chem. Soc.*, 1983, **105**, 3999–4008; (b) G. I. Nikishin, I. V. Svitanko and E. I. Troyansky, *J. Chem. Soc., Perkin Trans. 2*, 1983, 595–601; (c) G. Litwinienko, A. L. J. Beckwith and K. U. Ingold, *Chem. Soc. Rev.*, 2011, **40**, 2157; (d) M. Salamone and M. Bietti, *Acc. Chem. Res.*, 2015, **48**, 2895–2903.
- 19 (a) F. De Vleeschouwer, V. Van Speybroeck, M. Waroquier, P. Geerlings and F. De Proft, *Org. Lett.*, 2007, **9**, 2721–2724; (b) See also ref. 8p.

